CHALMERS
UNIVERSITY OF TECHNOLOGY

Robust PEDOT:PSS Wet-Spun Fibers for Thermoelectric Textiles

Macromolecular Materials and Engineering
www.mme-journal.de

Robust PEDOT:PSS Wet-Spun Fibers for Thermoelectric Textiles

Youngseok Kim, Anja Lund, Hyebin Noh, Anna I. Hofmann, Mariavittoria Craighero, Sozan Darabi, Sepideh Zokaei, Jae Il Park, Myung-Han Yoon, and Christian Müller**

To realize thermoelectric textiles that can convert body heat to electricity, fibers with excellent mechanical and thermoelectric properties are needed. Although poly(3,4-ethylenedioxythiophene):poly(styrene sulfonate) (PEDOT:PSS) is among the most promising organic thermoelectric materials, reports that explore its use for thermoelectric fibers are all but absent. Herein, the mechanical and thermoelectric properties of wet-spun PEDOT:PSS fibers are reported, and their use in energy-harvesting textiles is discussed. Wet-spinning into sulfuric acid results in water-stable semicrystalline fibers with a Young's modulus of up to 1.9 GPa, an electrical conductivity of 830 S cm^{-1}, and a thermoelectric power factor of 30 µV m^{-1} K^{-2}. Stretching beyond the yield point as well as repeated tensile deformation and bending leave the electrical properties of these fibers almost unaffected. The mechanical robustness/durability and excellent underwater stability of semicrystalline PEDOT:PSS fibers, combined with a promising thermoelectric performance, opens up their use in practical energy-harvesting textiles, as illustrated by an embroidered thermoelectric fabric module.

1. Introduction

The textile format is highly attractive for the design of truly wearable electronics that are set to transform health care, sports, and even fashion. Many applications require the integration of a myriad of miniaturized sensors, which would become considerably less cumbersome if each device was designed to operate autonomously without the need for batteries. A variety of electronic textiles (i.e., e-textiles) have been demonstrated that can generate power in situ by exploiting the photovoltaic,[1,2] piezoelectric,[3–6] triboelectric,[7,8] or thermoelectric effect.[9–13] Thermoelectric textiles are particularly intriguing because they would open up the possibility to harness body heat for electricity generation. At the same time, such textiles would allow to regulate the wearer's body temperature as they transport heat away from the skin to the typically colder surroundings. Alternatively, the same type of textile electronics could be used for local cooling when operating in reverse, i.e., they would function as a Peltier cooler.

The basic building blocks that are needed for the bottom-up design of a thermoelectric textile are conducting fibers or yarns. We argue that the use of polymer-based fibers is preferred since those will allow to replicate the form, feel, and function of the types of fabrics that we are familiar with through daily use. Conjugated polymers, which currently receive renewed attention as thermoelectric materials,[14–16] can be spun into fibers that display a Young's modulus (E) of 1–10 GPa,[17] which is a range of values that is common for many types of textile fibers.[18] At the same time, conjugated polymer fibers can display a conductivity (σ) of 10^2–10^3 S cm^{-1}.[17] The thermoelectric efficacy of conjugated polymers tends to increase with σ until values of 10^2–10^3 S cm^{-1} are reached, beyond which the thermal conductivity (κ) unduly increases. Overall, the thermoelectric figure-of-merit of a conjugated polymer, defined as $ZT = \alpha^2 \sigma T \kappa^{-1}$, where α is the Seebeck coefficient and T the absolute temperature, is likely optimized for the same range of electrical conductivities, and can reach a $ZT \approx 0.1$ in case of p-type organic materials.[19]

One of the most promising conjugated polymer-based thermoelectric materials is poly(3,4-ethylenedioxythiophene): poly(styrene sulfonate) (PEDOT:PSS). Intriguingly, PEDOT:PSS can be cast into free-standing tapes[20,21] and wet-spun into fibers,[22–28] which show good electrical conductivities and mechanical strength (e.g., fracture strain over 30%).[29] Despite the potential of PEDOT:PSS fibers toward thermoelectric applications, most previous research on PEDOT:PSS-based thermoelectric textiles with noticeable performance has been conducted by using composite fibers made of PEDOT:PSS and nanocarbon/inorganic materials or by coating mechanically robust fibers/yarns/fabrics with PEDOT:PSS. Recently, Liu et al. investigated the thermoelectric properties of fibers that had been

Y. Kim, H. Noh, J. I. Park, Prof. M.-H. Yoon
School of Materials Science and Engineering
Gwangju Institute of Science and Technology
Gwangju 61005, Republic of Korea
E-mail: mhyoon@gist.ac.kr

Dr. A. Lund, Dr. A. I. Hofmann, M. Craighero, S. Darabi, S. Zokaei, Prof. C. Müller
Department of Chemistry and Chemical Engineering
Chalmers University of Technology
Göteborg 41296, Sweden
E-mail: christian.muller@chalmers.se

S. Darabi, Prof. C. Müller
Wallenberg Wood Science Center
Chalmers University of Technology
Göteborg 41296, Sweden

The ORCID identification number(s) for the author(s) of this article can be found under https://doi.org/10.1002/mame.201900749.

DOI: 10.1002/mame.201900749

prepared from a PEDOT:PSS hydrogel; a $\alpha \approx 15$ μV K^{-1} and $\sigma \approx 173$ S cm^{-1} gave rise to a power factor $\alpha^2\sigma$ of ≈4 μW m^{-1} K^{-2}.[30] In conjunction with excellent electrical and thermoelectrical performance, fibers must display a high degree of fatigue resistance in order to withstand the considerable mechanical stresses encountered during textile manufacturing and daily use. Furthermore, fibers should be compatible with water immersion to facilitate post-treatment as well as permit laundering for multiple use. Nonetheless, the impact of mechanical deformation and water immersion on the (thermo)electrical behavior of PEDOT:PSS fibers has not been clarified, leading to the situation that there exist only few reports showing pure PEDOT:PSS fiber-based thermoelectric fibers with mechanical robustness, aqueous stability, and good (thermo)electrical characteristics.

Here, we investigate the mechanical properties and aqueous stability of PEDOT:PSS fibers prepared through wet-spinning into aqueous sulfuric acid (SA). Owing to the removal of undesired PSS and the formation of semicrystalline PEDOT domains, a promising electrical conductivity of up to 830 S cm^{-1} and thermoelectric power factor $\alpha^2\sigma$ of up to 30 μW m^{-1} K^{-2} are paired with a Young's modulus of 1.9 GPa and a strain at break of 40%. These fibers display an exceptional resilience against repeated tensile and bending deformation as well as exposure to water, which paves a way toward practical thermoelectric textiles, as illustrated by a 10-leg embroidered fabric module.

2. Results and Discussion

We prepared up to 10 cm long semicrystalline fibers by wet-spinning of an aqueous PEDOT:PSS dispersion into aqueous SA, where as-spun fibers remained for 6 h, followed by rinsing with deionized water and finally drying in air (**Scheme 1**). To obtain a spinning dope with a sufficiently high viscosity, we removed a certain portion of the water from a commercial PEDOT:PSS dispersion through solvent evaporation prior to spinning, which resulted in a solid content of 2.2–2.6%. We chose sulfuric acid as the coagulation bath because it is a good solvent for PSS, but a nonsolvent for PEDOT.[31,32] The acid, which has a high dielectric constant, reduces the electrostatic interaction between PSS and PEDOT, and therefore facilitates the removal of both PSS and water as the fiber enters the coagulation bath.[22] We varied the composition of the coagulation bath by diluting concentrated sulfuric acid (EP grade, ≈95%) with different amounts of deionized water, which allowed us to selectively remove PSS from the spinning dope. X-ray photoelectron spectroscopy (XPS) of pristine PEDOT:PSS and two representative fibers (i.e., coagulated in 45% and 95% SA) confirms that the acid concentration had a prominent impact on the ratio of PEDOT to PSS, as indicated by the different strengths of the S 2p doublets that can be assigned to S's in sulfonate (i.e., PSS) or thiophene (i.e., PEDOT) (**Figure 1**a).[33] We observe one broad signal around 169 eV from PSS, whose relative strength decreases with acid concentration, confirming that a sizable fraction of the polyanion (i.e., PSS) is removed

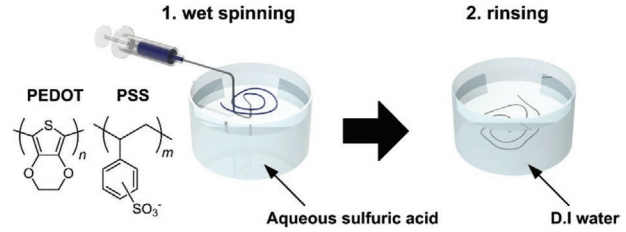

Scheme 1. Schematics of wet-spinning: 1) aqueous PEDOT:PSS dispersion is wet-spun into sulfuric acid coagulation bath and 2) the fiber remains in the coagulation bath for 6 h and is finally rinsed with deionized water.

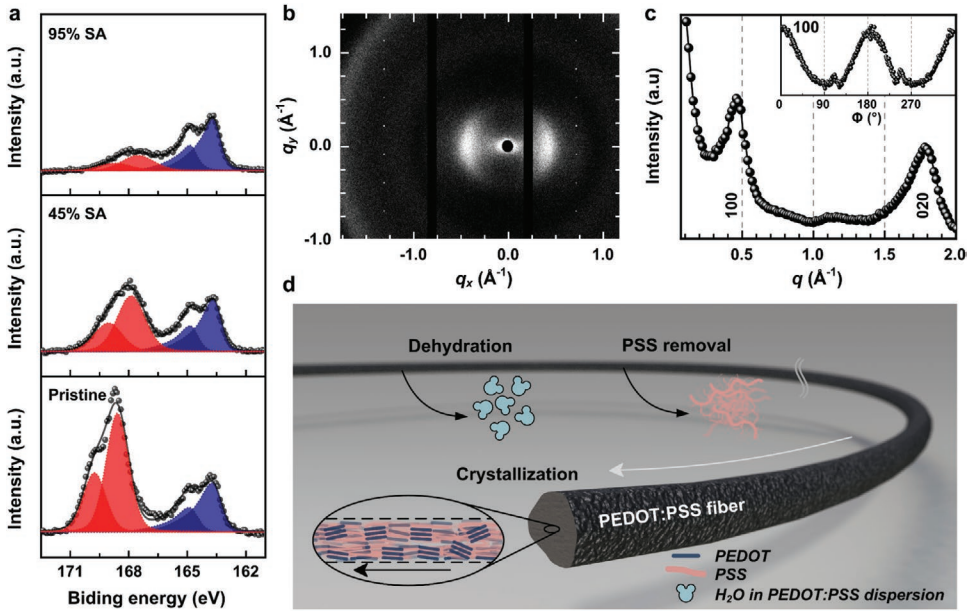

Figure 1. Compositional and structural examination of PEDOT:PSS fibers. a) XPS spectra of pulverized PEDOT:PSS fibers wet-spun into 95% and 45% SA, and a pristine PEDOT:PSS film, and its fitted curves using an asymmetric model (line). b) X-ray diffraction pattern. c) Diffractogram showing the radial intensity distribution and (inset) angular distribution of the q_{100} diffraction. d) A schematic of the mechanism of wet-spinning in sulfuric acid.

Table 1. Mechanical and electrical properties of PEDOT:PSS fibers: cross-sectional area A ($n = 4$), Young's modulus E ($n = 3$), strain at break ε_{break} ($n = 3$), electrical conductivity σ ($n = 4$), Seebeck coefficient α ($n = 1$), and thermoelectrical power factor $\alpha^2\sigma$; n = number of measured samples.

Coagulation bath % sulfuric acid	A [10^3 μm^2]	E [GPa]	ε_{break} [%]	σ [S cm^{-1}]	α [μV K^{-1}]	$\alpha^2\sigma$ [μW m^{-1} K^{-2}]
35	3.2 ± 0.6	0.5 ± 0.1	83	92 ± 3	17 ± 1	2.7 ± 0.3
45	8.6 ± 0.7	1.1 ± 0.2	34	245 ± 6	15 ± 1	5.5 ± 0.9
65	1.9 ± 0.1	0.7 ± 0.1	43	450 ± 10	15 ± 1	10.1 ± 1.4
95	0.9 ± 0.1	1.9 ± 0.2	40	830 ± 18	19 ± 1	30.0 ± 3.4

during immersion of the fibers in the coagulation bath of 95% SA. Instead, PEDOT yields a distinct doublet at 164 eV that does not change shape. Note that the asymmetric tails of the PEDOT doublet originate from doped PEDOT chains.[34] Careful fitting of the XPS spectra of fibers prepared through coagulation with 95% SA, where the PSS signal is sufficiently small, yielded a [EDOT] to [SS] ratio of about ≈2:1 (68% PEDOT). It is noteworthy that such PEDOT rich fibers lead to reduced fiber swelling and, thereby, enhanced mechanical stability in water (see below).

In a first set of experiments, we characterized the electrical conductivity (σ) of the wet-spun PEDOT:PSS fibers. As anticipated, σ markedly increased by almost one order of magnitude from 92 to 830 S cm^{-1} with increasing PEDOT content as a result of removal of PSS during coagulation (**Table 1**). Note that in the case of PEDOT:PSS thin films, the removal of PSS with sulfuric acid tends to strongly increase the degree of crystalline order of the remaining PEDOT, and lead to a marked texture with preferential edge-on orientation of PEDOT chains as confirmed by grazing incidence wide-angle X-ray scattering (GIWAXS).[32,35] We employed transmission wide-angle X-ray scattering (WAXS) to examine the structural order of fibers produced with a 95% SA coagulation bath. Prominent diffractions at $q_{100} \approx 0.45$ Å^{-1} and $q_{020} \approx 1.75$ Å^{-1} indicate that the fibers are semicrystalline (Figure 1b,c). Further, fiber diffraction patterns indicate a moderate degree of alignment of PEDOT chains along the fiber axis with a Herman's orientation factor $f_{100} \approx 0.15$ for the prominent equatorial 100 diffraction (Figure 1c inset; $f = 1$ for perfect alignment parallel to the fiber axis). As depicted in the scheme (Figure 1d), injection of the PEDOT:PSS dispersion into the sulfuric acid causes the removal of water molecules and loosely bound PSS chains, leading to semicrystalline PEDOT:PSS fibers with moderate orientation along the fiber axis.

Tensile tests allowed us to compare the mechanical properties of PEDOT:PSS fibers. The Young's modulus (E) increased from 0.5 to 1.9 GPa with increasing sulfuric acid concentration (Table 1). Likewise, we observed a reduction in the strain at break from $\varepsilon_{break} \approx 80\%$ to 40% upon removal of PSS. The yield point remained unaffected with a yield strain (ε_{yield}) of ≈5% (**Figure 2**a,b; Figure S1, Supporting Information). We monitored the electrical resistance of fibers during stretching in order to explore the impact of plastic deformation beyond the yield point. Strikingly, the electrical resistance of PEDOT:PSS microfibers display a high tolerance to mechanical deformation until fracture. Considering the fiber thinning during tensile stretching due to the Poisson effect, it is clear that the dimension-normalized electrical conductivity is increased by stretching, which can be attributed to the alignment of PEDOT chains induced by tensile strain (Figure 2a,b).[13,29] To further examine how PEDOT:PSS fibers respond to repeated mechanical stress, we carried out a series of cyclic tensile deformation and bending tests. Cyclic tensile deformation with a maximum strain of 5%, i.e., at ε_{yield}, only causes a marginal (<10%) increase in resistance after 100 cycles (Figure 2c). Moreover, repeated bending to a diameter of 8.3 mm resulted in only minimal change in resistance even after 1000 cycles, which indicates a high degree of fatigue resilience (Figure 2d). Evidently, our PEDOT:PSS fibers are characterized by a high degree of robustness and are able to withstand repeated deformation without significant change in their electrical properties, which can be attributed to the semicrystalline fiber microstructure. Therefore, we were readily able to tie a knot into a PEDOT:PSS fiber (Figure 2e). All of the abovementioned results suggest that semicrystalline PEDOT:PSS fibers are suitable for the integration into a fabric by conventional knitting or weaving.

Another important requirement for e-textile devices is structural stability in the presence of water so that they can withstand perspiration and laundry. Even though PEDOT:PSS is chemically stable in aqueous environment, its solid form readily absorbs water owing to the hydrophilic nature of PSS, leading to substantial swelling.[32] To study the geometrical behavior of our PEDOT:PSS fibers in aqueous environment, we performed a swelling test using a micromachined fluidic structure, as described in the following (**Figure 3**a). i) At first, the grooves for fluid (width: 1 mm, depth: 1 mm) and capillary channels (width: 0.25 mm, depth: 1 mm) were defined on glass substrates. Then, a fiber was embedded into the fluid channel. ii) The top of the glass substrate was sealed by attaching a polydimethylsiloxane (PDMS) elastomer block. iii) Subsequently, deionized water was injected through the capillary channel and, then, spread into the fluidic channel via capillary force. Finally, the geometrical change of a given fiber after water immersion (5 min) was monitored by optical microscopy (Figure 3b). Since the control wet-spun PEDOT:PSS fibers prepared in an acetone coagulation bath exhibit very small cross-sectional areas (≈800 μm^2) due to the inefficient coagulation, the swelling test was conducted in the smaller-volume fluid channel (width: 0.5 mm, no capillary channel). As summarized in Figure 3c, the PEDOT:PSS fibers wet-spun into 95% and 45% SA only expand by 1.7 and 7.1 times, respectively, in volume, while the fiber wet-spun into acetone dramatically expands by 44 times in volume. Severe swelling in polar solvent-treated PEDOT:PSS fibers is mainly due to the excessive content of residual PSS, unlike those prepared in an aqueous sulfuric acid, which contain much less PSS (Figure 1a). Note also that the material is

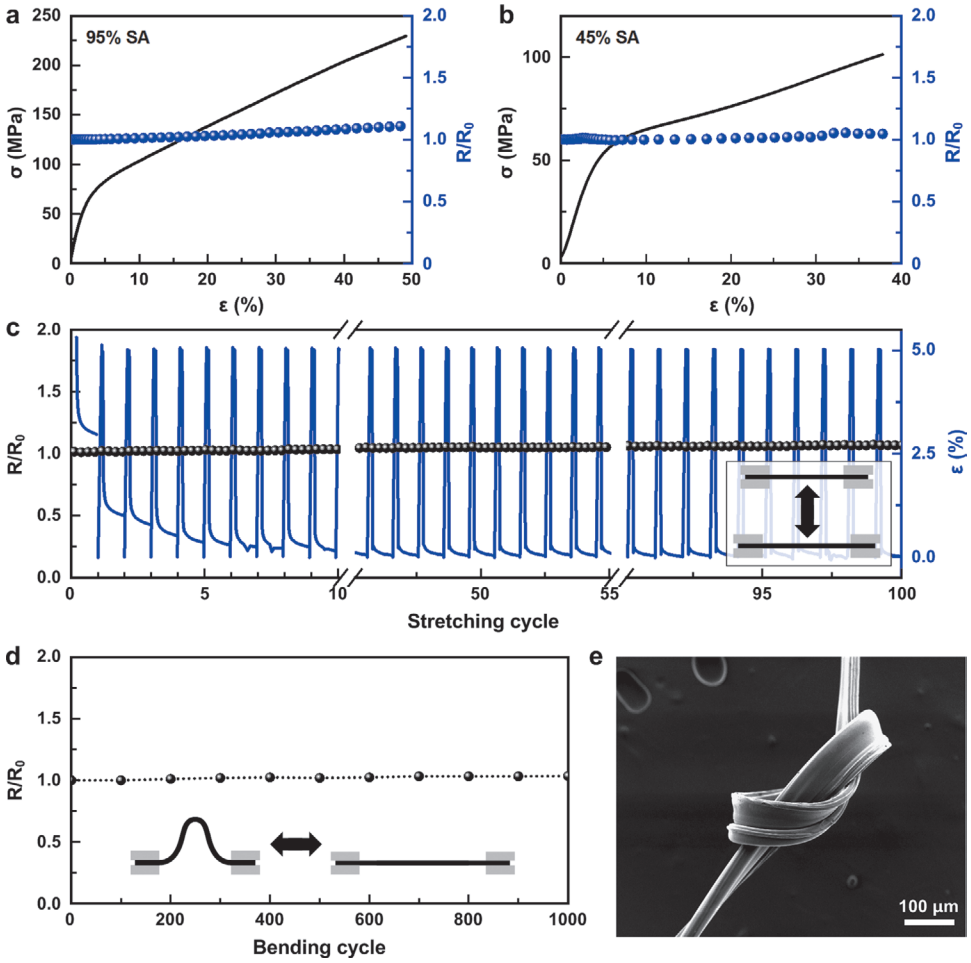

Figure 2. Mechanical properties of PEDOT:PSS fibers. a,b) Stress–strain curves and relative electrical resistance (R/R_0) of 95% SA- and 45% SA-treated fibers, where $R_0 = R(\varepsilon = 0)$. c) R/R_0 recorded during dynamic tensile deformation of a fiber (95% SA) with a maximum strain of 5% with a schematic of tensile deformation (inset). d) R/R_0 measured after repeated bending of a fiber (95% SA) with a bending diameter of 8.3 mm. (Inset) A schematic of fiber bending. e) An SEM image of a fiber tied into a knot (95% SA).

aligned slightly along the fiber direction (see also Figure 1b,c), so that the swelling ratios measured along the fiber axis are lower than those along the axial direction.[36]

Next, we examined the thermoelectric performance of PEDOT:PSS fibers as a function of the sulfuric acid concentration in the coagulation bath. We only observed slight variations in the Seebeck coefficient (α) from 15 to 19 µV K^{-1}. As a result, the power factor ($\alpha^2\sigma$) considerably increased along with σ from 3 to 30 µW m^{-1} K^{-2} upon changing the sulfuric acid concentration from 35% to 95% (Table 1 and **Figure 4**). To estimate the thermal conductivity we used the Wiedemann–Franz law and the Sommerfeld value for the Lorenz number $L = 2.44 \cdot 10^{-8}$ W Ω K^{-2}, so that $\lambda = \lambda_{ph} + \sigma LT$. Liu et al reported a value of $\lambda_{ph} \approx 0.64$ W m^{-1} K^{-1} for the phonon part of the in-plane thermal conductivity of drop-cast PEDOT:PSS films, which showed considerable anisotropy.[37] Using the same value, we estimate a thermal conductivity of $\lambda \approx 1.2$ W m^{-1} K^{-1} for the most conductive PEDOT:PSS fibers ($\sigma \approx 830$ S cm^{-1}), which we consider to be a lower bound. Overall, we obtain a figure-of-merit (ZT) of up to $7 \cdot 10^{-3}$ at room temperature.

A number of previous publications indicate that the power factor of PEDOT:tosylate can be improved by chemical dedoping with tetrakis(dimethylamino)ethylene (TDAE) or polyethyleneimine (PEI).[38,39] Inspired by these reports and the good aqueous stability of our PEDOT:PSS fibers, we studied their thermoelectric properties upon dedoping through the immersion in aqueous solutions of PEI (**Figure 5**a). The PEI-dedoped PEDOT:PSS fibers were collected after a simple solution-dipping process using various PEI solutions (0.01–100 g L^{-1}). The N 1s peak in XPS spectra which corresponds to amine groups in PEI suggests that the treatment with higher concentration of positively charged PEI solution leads to a higher concentration of the reducing agent due to the electrostatic interaction with negatively charged PSS (Figure 5b). In parallel, fibers prepared with a coagulation bath of 95% SA exhibit a lower PEI content than those prepared with a coagulation bath of 45% SA. We argue that the residual PSS content impacts the ability of fibers to take up PEI since the hydrophilicity of PSS facilitates ingression of water. Also, we note a reduction in the asymmetry of the S 2p doublets assigned to PEDOT (Figure S2, Supporting Information), which is

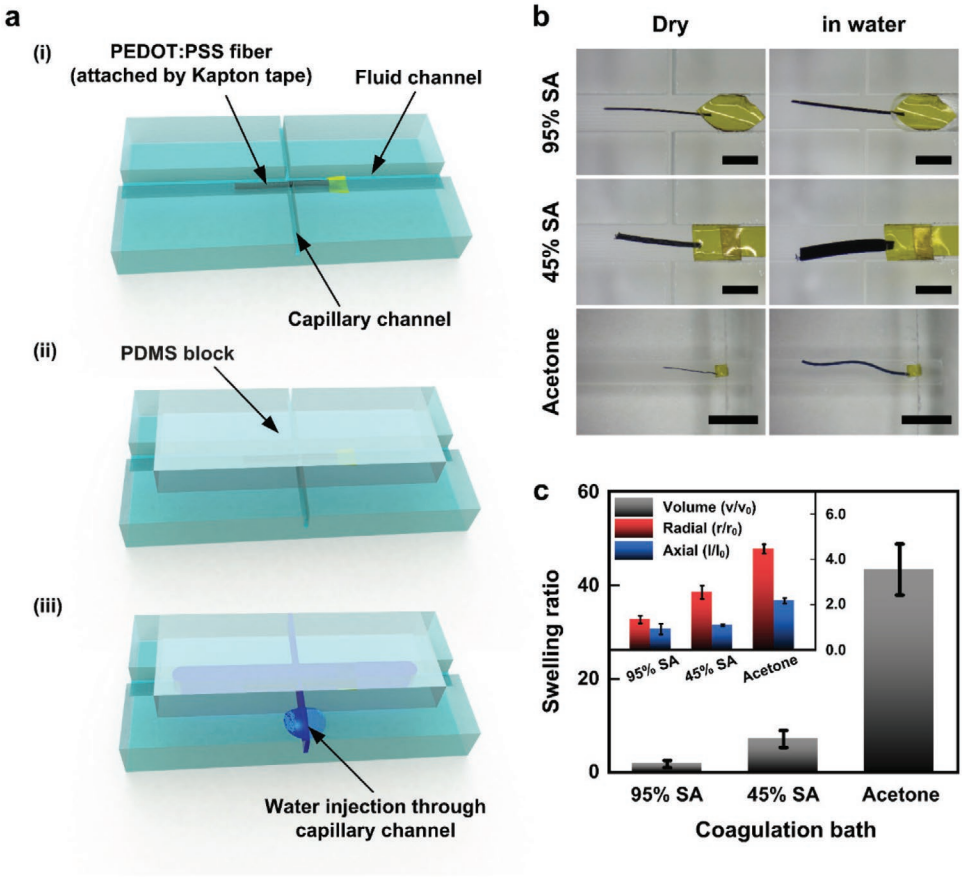

Figure 3. Swelling of PEDOT:PSS fibers in water. a) Schematics of the swelling test using a micromachined fluidic channel. b) Photographs of fibers (prepared with coagulation bath of 95% SA, 45% SA, and acetone) in dry (left) and water immersion states (right). All scale bars denote 1 mm. c) Volume swelling and (inset) axial/radial swelling ratios between wet and dry fibers.

consistent with a lower charge carrier density.[34,40] We also carried out energy-dispersive X-ray spectroscopy (EDX) to examine the distribution of PEI throughout the bulk of the fiber. EDX spectra indicate a uniform distribution of PEI throughout dedoped fibers (Figure S3, Supporting Information).

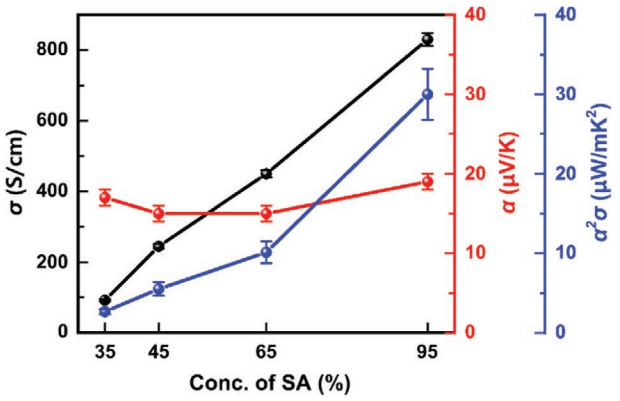

Figure 4. Thermoelectric properties of PEDOT:PSS fibers. The plots of electrical conductivity (σ), Seebeck coefficient (α), and power factor ($\alpha^2\sigma$) of fibers wet-spun into coagulation baths with a sulfuric acid concentration ranging from 35% to 95%.

Despite the uptake of PEI by the bulk fibers, we observed increased mechanical properties upon dedoping, for instance, an increase in Young's modulus from 1.9 to 4 GPa for fibers wet-spun into 95% SA (Figure S4, Supporting Information). The electrical conductivity strongly decreased upon dedoping (Figure 5c), while the Seebeck coefficient only slightly increased, reaching values of ≈30 μV K^{-1} (Figure 5d). Overall, the power factor remained the same or decreased upon dedoping with various concentrations of PEI, and therefore we chose to carry out our remaining experiments with neat fibers (Figure 5e).

In a final set of experiments, we constructed a small thermoelectric module to demonstrate that energy-harvesting textiles can be fabricated with our mechanically robust PEDOT:PSS fibers with promising electrical and thermoelectric characteristics. We chose to work with the most conductive ($\sigma \approx$ 830 S cm^{-1}) fibers to minimize the internal resistance of the module. The in-plane device consisted of $n_e = 10$ thermoelectric elements, connected in series, that each comprised one PEDOT:PSS fiber and one silver plated nylon yarn. We successfully embroidered the fibers onto a 300 μm thick piece of cotton fabric and made electrical connections with silver paste (**Figure 6**a,b). Application of a temperature difference ΔT across the in-plane device is expected to give rise to an output voltage $V_{out} = n_e \cdot (\alpha_p - \alpha_{Ag}) \cdot \Delta T$ where $\alpha_p = 19$ μV K^{-1} (Table 1) and

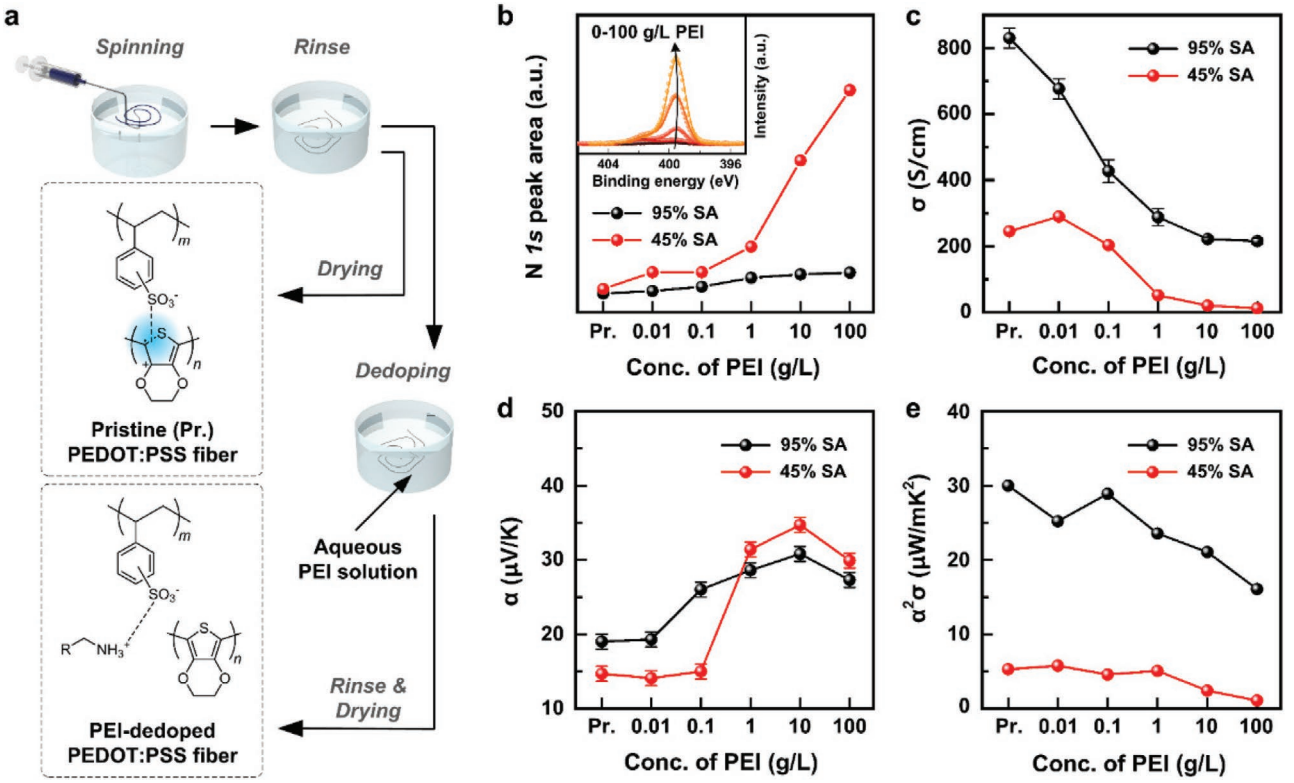

Figure 5. XPS spectra and electrical/thermoelectric properties of chemically dedoped PEDOT:PSS fibers. a) Schematics of the solution-based dedoping method using aqueous PEI solution. b) Integrated intensity of the N 1s peak of fibers (95% and 45% SA) dedoped using PEI solutions with concentration 0–100 g L^{-1}. (Inset) N 1s peak profiles of fibers wet-spun into 95% SA after dedoping with various PEI concentrations. c) Electrical conductivity (σ), d) Seebeck coefficient (α), and e) power factor ($\alpha^2\sigma$) of fibers (95% and 45% SA) dedoped using PEI solutions with concentration 0–100 g L^{-1}.

$\alpha_{Ag} = 0.3$ μV K^{-1} are the Seebeck coefficients of the PEDOT:PSS fiber and silver plated yarn, respectively. We measured a value of $V_{out}/\Delta T \approx 7.9$ mV for a temperature gradient of $\Delta T \approx 40$ °C (Figure 6c), which is in good agreement with our predicted value of 7.2 mV. The internal resistance of the module largely scales with the length $L = 2.5$ cm of the p-type PEDOT:PSS fiber legs according to $R_{in} \propto n_e L/(\sigma A)$, where A is the cross-sectional area of the fibers (Table 1). We measured an internal resistance of $R_{in} \approx 10$ kΩ, close to the predicted resistance of the 10 p-type legs of 3 kΩ. The maximum power that can be produced by the device is given by $P_{max} = V_{out}^2/(4R_{in})$, and is achieved under load matching conditions, $R_{load} = R_{in}$. We used a source/measure unit as an active load that acts as a variable current sink to measure the output power produced as a function of applied load, and find for $\Delta T \approx 40$ °C and $I_{load} = 0.7$ μA a value of $P_{max} \approx 2.8$ nW (Figure 6d), again consistent with our prediction of 1.6 nW.

3. Conclusions

We have demonstrated that wet-spinning of PEDOT:PSS into sulfuric acid is suitable for the preparation of robust conducting polymer fibers that combine promising mechanical/environmental durability and electrical/thermoelectric performance. In conjunction with excellent stability upon water exposure, semicrystalline PEDOT:PSS fibers featured a Young's modulus of 0.5–1.9 GPa and a high degree of mechanical robustness and excellent fatigue resistance over at least 1000 bending cycles and 100 tensile deformation cycles up to the yield point. A promising electrical conductivity of up to 830 S cm^{-1}, paired with a Seebeck coefficient of 15–30 μV K^{-1}, which could be easily tuned by simple dedoping with PEI, gave rise to a power factor of up to 30 μW m^{-1} K^{-2}. Finally, we constructed an embroidered thermoelectric module using our pure PEDOT:PSS fibers, which illustrates their usefulness for the construction of energy-harvesting textiles with promising thermoelectric performance.

4. Experimental Section

Materials: Aqueous PEDOT:PSS solution (PH1000 1.1–1.3 wt% solid content) was purchased from Heraeus. Sulfuric acid (EP grade; concentrated ≈95%) was purchased from Duksan Chemicals (South Korea) and used as received. PEI with a weight-average molecular weight (M_w) of ≈25 kg mol^{-1} was purchased from Sigma-Aldrich and used as received. The silver plated polyamide yarn (HC12) was purchased from MADEIRA Garnfabrik (Germany).

Wet-Spinning and Dedoping: As-received PEDOT:PSS dispersion was concentrated to increase its viscosity, and then filtered with a syringe filter (Satorius, 17593). For wet-spinning, the resulting dispersion was injected into a sulfuric acid coagulation bath using 18G stainless steel needles and a syringe pump (New Era, NE-1000) with a pumping rate of 50 mL h^{-1}. Then, as-spun PEDOT:PSS fibers were left in the same sulfuric acid coagulation bath for 6 h while the whole bath was

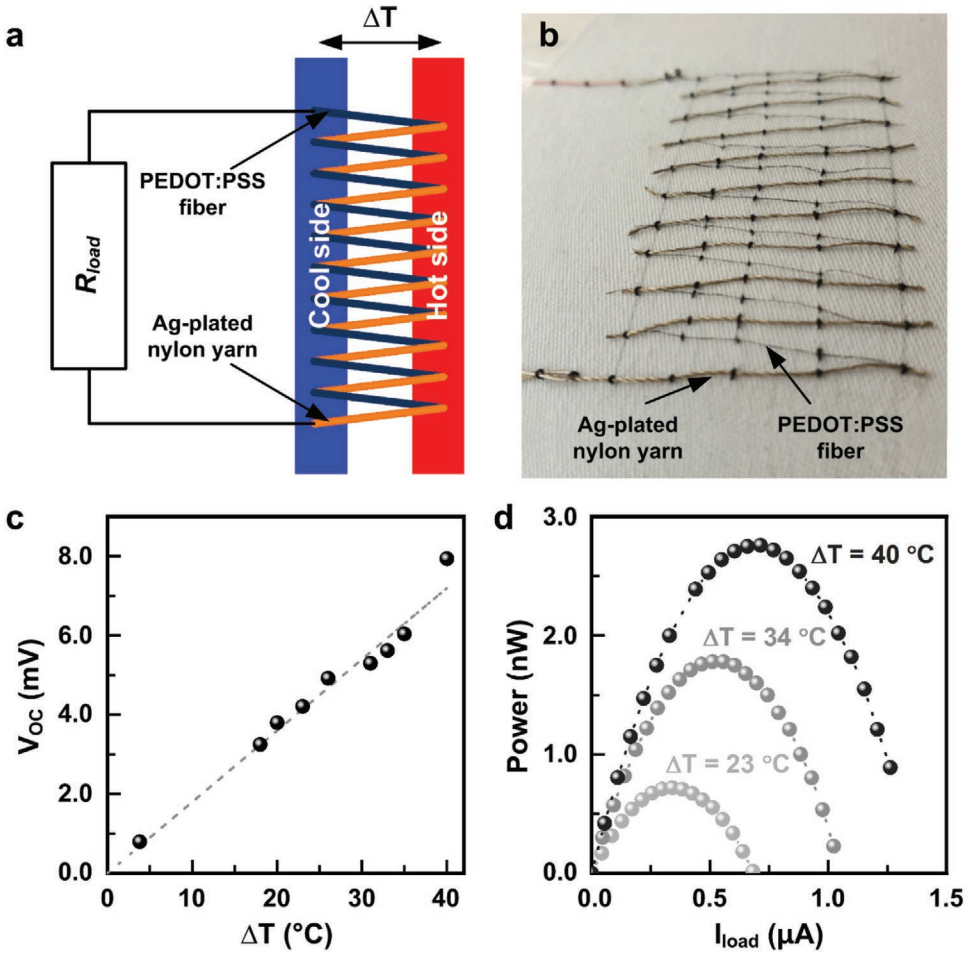

Figure 6. Embroidered thermoelectric module. a) Schematic and b) photograph of PEDOT:PSS-fiber embroidered thermoelectric module consisting of ten elements (each comprising one p-type PEDOT:PSS fiber and one silver plated nylon yarn). c) Open circuit voltage (V_{oc}) as a function of temperature difference (ΔT) with respect to the cold end (24 °C). The measured V_{oc} data (symbols) closely follow the predicted (dashed line) linear relationship with ΔT. d) The plot of power P as a function of load current (I_{load}) with three temperature differences (23, 34, and 40 °C).

continuously shaken, followed by washing the fibers in deionized water. For dedoping, fibers were immersed in an aqueous PEI bath (0.01–100 g L^{-1}) overnight. Then, dedoped PEDOT:PSS fibers were rinsed with deionized water, and dried by hanging in air for 1 h.

Optical Microscopy: Optical microscopy was carried out with an Olympus BX51 microscope. Fiber samples were fixated in a cold-mount resin (R&B Inc., CM-ERH-Thin) and polished (Allied High Tech Products, M-PREP 5) to reveal the cross-section. The cross-sectional area was determined through image processing (ImageJ) of optical microscopy images.

XPS: XPS was done with a K-Alpha XPS instrument from Thermo Fisher Scientific. Samples were prepared by pulverizing frozen PEDOT:PSS fibers in liquid nitrogen using a mortar and pestle. The degree of asymmetry is calculated by the following equation

$$\text{Degree of asymmetry}\,(\%) = \frac{A_{\text{asymmetry}} - A_{\text{symmetry}}}{A_{\text{asymmetry}}} \times 100 \quad (1)$$

where $A_{\text{asymmetry}}$ and A_{symmetry} are measured peak areas of fitted curves by using asymmetric/symmetric fitting models, respectively. All the spectra were normalized by the S 2p peak of PEDOT whose original content is identical during coagulation and dedoping.

Scanning Electron Microscopy (SEM) and EDX: SEM and EDX were carried out at 3 and 5 kV, respectively, using a JEOL 7800F Prime SEM. Samples were freeze-fractured prior to EDX analysis.

WAXS: WAXS diffractograms were obtained using a Mat:Nordic instrument from SAXSLAB equipped with a Rigaku 003+ high brilliance micro focus Cu-radiation source (wavelength = 1.5406 Å) and a Pilatus 300K detector placed at a distance of 88.6 mm from the sample. The Herman's orientation factor f for angular distribution of the prominent equatorial diffraction at 0.45 $Å^{-1}$ was calculated as described in ref. [41].

Mechanical Characterization: Tensile testing and cyclic tensile deformation were performed using a Q800 Dynamic Mechanical Analyzer (DMA) from TA Instruments. For stress/strain measurements, fibers were subjected to a ramped force of 0.5 N min^{-1} at room temperature. Cyclic tensile deformation was done by subjecting the fiber to a strain of 5% for 6 s followed by a recovery time of 30 s. This cycle was repeated 100 times. During mechanical testing, the electrical resistance was recorded with a Keysight U1253B multimeter using a two-point probe configuration. Bending resilience was probed with a custom-built LEGO setup[42] that allowed to repeatedly bend a fiber to a diameter of 8.3 mm. The electrical resistance of the fiber was measured once per 100 bending cycles using a Keithley 2400 source meter.

Swelling Ratio: A fluidic channel (width: 1 mm; depth: 1 mm) with a vertically located capillary channel (width: 0.25 mm; depth: 1 mm) was micromachined on glass substrates (soda lime glass, thickness: 50 mm) using a dicing saw (Disco, DAD320). Then, one end of a PEDOT:PSS fiber (length: ≈2 mm) was inserted into the fluidic channel and fixed with Kapton tape, and the upper side of the fluidic channel was sealed with a slab of PDMS (Corning, Sylgard 184). To monitor the increase

in diameter after water-immersion, deionized water was injected into the capillary channels, and the fibers were exposed to water for 5 min. Then, to calculate the swelling ratios, the diameters of dry and swollen PEDOT:PSS fibers were measured with an optical microscope (Sunny Optical Technology, SZN45T). The average swelling ratio was obtained from four different fibers.

Electrical Characterization: The electrical resistance of fibers was measured using a source meter (Keithley 2400) in four-point probe configuration. A current bias of 100 µA was applied between the outer contacts, and the voltage drop between the two inner contacts, placed 5 mm apart, was recorded. The conductivity was calculated using the measured resistance value and cross-sectional area (optical microscopy). Seebeck coefficients were measured at 300 K with a SB1000 instrument equipped with a K2000 temperature controller from MMR Technologies, using a thermal load of 1–2 K and a constantan wire as an internal reference. Samples of about 4 mm length were mounted on the sample stage using silver paint (Agar Silver Paint, G302). To characterize the thermoelectric module, an in-plane temperature gradient was applied by placing one end on a hot plate and the other end on a room-tempered metal plate. The generated voltage was measured with a Keithley 2400 source/measure unit and temperatures were recorded using two surface mounted K-type temperature probes (Omega Engineering). Highly conducting silver paint (Agar Silver Paint, G302) was added to all electrical contact points of the textile module.

Supporting Information

Supporting Information is available from the Wiley Online Library or from the author.

Acknowledgements

The authors gratefully acknowledge the financial support from the Swedish Research Council (Vetenskapsrådet) through grant number 2016-06146, the Knut and Alice Wallenberg Foundation through a Wallenberg Academy Fellowship, and the H2020 European Research Council (ERC) under grant agreement number 637624. This research was also supported by the Basic Science Research Program through the National Research Foundation of Korea (NRF) funded by the Ministry of Science and ICT (NRF-2017R1A2B4003873 and NRF-2018M3A7B4070988) and the GIST Research Institute in 2019. Part of the work was performed at the Chalmers Materials Analysis Laboratory (CMAL).

Conflict of Interest

The authors declare no conflict of interest.

Keywords

conducting polymer fibers, electronic textiles, thermoelectric textiles, wet spinning

Received: November 4, 2019
Revised: December 17, 2019
Published online: February 24, 2020

[1] H. Peng, *Fiber-Shaped Energy Harvesting and Storage Devices*, Nanostructure Science and Technology, Springer-Verlag, Berlin **2015**.
[2] Z. Wen, M.-H. Yeh, H. Guo, J. Wang, Y. Zi, W. Xu, J. Deng, L. Zhu, X. Wang, C. Hu, L. Zhu, X. Sun, Z. L. Wang, *Sci. Adv.* **2016**, *2*, e1600097.
[3] A. Lund, K. Rundqvist, E. Nilsson, L. Yu, B. Hagström, C. Müller, *npj Flexible Electron.* **2018**, *2*, 9.
[4] J. Chang, M. Dommer, C. Chang, L. Lin, *Nano Energy* **2012**, *1*, 356.
[5] L. Persano, C. Dagdeviren, Y. Su, Y. Zhang, S. Girardo, D. Pisignano, Y. Huang, J. A. Rogers, *Nat. Commun.* **2013**, *4*, 1633.
[6] N. Soin, T. H. Shah, S. C. Anand, J. Geng, W. Pornwannachai, P. Mandal, D. Reid, S. Sharma, R. L. Hadimani, D. V. Bayramol, E. Siores, *Energy Environ. Sci.* **2014**, *7*, 1670.
[7] J. Chen, Y. Huang, N. Zhang, H. Zou, R. Liu, C. Tao, X. Fan, Z. L. Wang, *Nat. Energy* **2016**, *1*, 16138.
[8] K. N. Kim, J. Chun, J. W. Kim, K. Y. Lee, J.-U. Park, S.-W. Kim, Z. L. Wang, J. M. Baik, *ACS Nano* **2015**, *9*, 6394.
[9] Y. Du, K. Cai, S. Chen, H. Wang, S. Z. Shen, R. Donelson, T. Lin, *Sci. Rep.* **2015**, *5*, 6411.
[10] J. A. Lee, A. E. Aliev, J. S. Bykova, M. J. de Andrade, D. Kim, H. J. Sim, X. Lepró, A. A. Zakhidov, J.-B. Lee, G. M. Spinks, S. Roth, S. J. Kim, R. H. Baughman, *Adv. Mater.* **2016**, *28*, 5038.
[11] J. D. Ryan, D. A. Mengistie, R. Gabrielsson, A. Lund, C. Müller, *ACS Appl. Mater. Interfaces* **2017**, *9*, 9045.
[12] J. D. Ryan, A. Lund, A. I. Hofmann, R. Kroon, R. Sarabia-Riquelme, M. C. Weisenberger, C. Müller, *ACS Appl. Energy Mater.* **2018**, *1*, 2934.
[13] R. Sarabia-Riquelme, M. Shahi, J. W. Brill, M. C. Weisenberger, *ACS Appl. Polym. Mater.* **2019**, *1*, 2157.
[14] R. Kroon, D. A. Mengistie, D. Kiefer, J. Hynynen, J. D. Ryan, L. Yu, C. Müller, *Chem. Soc. Rev.* **2016**, *45*, 6147.
[15] B. Russ, A. Glaudell, J. J. Urban, M. L. Chabinyc, R. A. Segalman, *Nat. Rev. Mater.* **2016**, *1*, 16050.
[16] O. Bubnova, X. Crispin, *Energy Environ. Sci.* **2012**, *5*, 9345.
[17] A. Lund, N. M. van der Velden, N.-K. Persson, M. M. Hamedi, C. Müller, *Mater. Sci. Eng., R* **2018**, *126*, 1.
[18] H. Eberle, *Clothing Technology: From Fibre to Fashion*, Verlag Europa-Lehrmittel Nourney, Vollmer, Haan, Germany **2008**.
[19] D. Beretta, N. Neophytou, J. M. Hodges, M. G. Kanatzidis, D. Narducci, M. Martin- Gonzalez, M. Beekman, B. Balke, G. Cerretti, W. Tremel, A. Zevalkink, A. I. Hofmann, C. Müller, B. Dörling, M. Campoy-Quiles, M. Caironi, *Mater. Sci. Eng., R* **2018**, *138*, 100501.
[20] D. A. Mengistie, C.-H. Chen, K. M. Boopathi, F. W. Pranoto, L.-J. Li, C.-W. Chu, *ACS Appl. Mater. Interfaces* **2015**, *7*, 94.
[21] Z. Li, H. Sun, C.-L. Hsiao, Y. Yao, Y. Xiao, M. Shahi, Y. Jin, A. Cruce, X. Liu, Y. Jiang, W. Meng, F. Qin, T. Ederth, S. Fabiano, W. M. Chen, X. Lu, J. Birch, J. W. Brill, Y. Zhou, X. Crispin, F. Zhang, *Adv. Electron. Mater.* **2018**, *4*, 1700496.
[22] Y. Kim, T. Lim, C.-H. Kim, C. S. Yeo, K. Seo, S.-M. Kim, J. Kim, S. Y. Park, S. Ju, M.-H. Yoon, *NPG Asia Mater.* **2018**, *10*, 1086.
[23] R. Jalili, J. M. Razal, P. C. Innis, G. G. Wallace, *Adv. Funct. Mater.* **2011**, *21*, 3363.
[24] D. Yuan, B. Li, J. Cheng, Q. Guan, Z. Wang, W. Ni, C. Li, H. Liu, B. Wang, *J. Mater. Chem. A* **2016**, *4*, 11616.
[25] J. Zhou, E. Q. Li, R. Li, X. Xu, I. A. Ventura, A. Moussawi, D. H. Anjum, M. N. Hedhili, D.-M. Smilgies, G. Lubineau, S. T. Thoroddsen, *J. Mater. Chem. C* **2015**, *3*, 2528.
[26] H. Okuzaki, Y. Harashina, H. Yan, *Eur. Polym. J.* **2009**, *45*, 256.
[27] H. Okuzaki, M. Ishihara, *Macromol. Rapid Commun.* **2003**, *24*, 261.
[28] G. Tian, J. Zhou, Y. Xin, R. Tao, G. Jin, G. Lubineau, *Polymer* **2019**, *177*, 189.
[29] J. Zhang, S. Seyedin, S. Qin, P. A. Lynch, Z. Wang, W. Yang, X. Wang, J. M. Razal, *J. Mater. Chem. A* **2019**, *7*, 6401.
[30] J. Liu, Y. Jia, Q. Jiang, F. Jiang, C. Li, X. Wang, P. Liu, P. Liu, F. Hu, Y. Du, J. Xu, *ACS Appl. Mater. Interfaces* **2018**, *10*, 44033.
[31] S.-M. Kim, N. Kim, Y. Kim, M.-S. Baik, M. Yoo, D. Kim, W.-J. Lee, D.-H. Kang, S. Kim, K. Lee, M.-H. Yoon, *NPG Asia Mater.* **2018**, *10*, 255.

[32] S.-M. Kim, C.-H. Kim, Y. Kim, N. Kim, W.-J. Lee, E.-H. Lee, D. Kim, S. Park, K. Lee, J. Rivnay, M.-H. Yoon, *Nat. Commun.* **2018**, *9*, 3858.
[33] A. Elschner, S. Kirchmeyer, W. Lovenich, U. Merker, K. Reuter, *PEDOT: Principles and Applications of an Intrinsically Conductive Polymer*, CRC Press, Boca Raton, FL.
[34] T. A. Skotheim, J. Reynolds, *Conjugated Polymers: Theory, Synthesis, Properties, and Characterization*, CRC Press, Boca Raton, FL.
[35] C. M. Palumbiny, F. Liu, T. P. Russell, A. Hexemer, C. Wang, P. Müller-Buschbaum, *Adv. Mater.* **2015**, *27*, 3391.
[36] B. Lu, H. Yuk, S. Lin, N. Jian, K. Qu, J. Xu, X. Zhao, *Nat. Commun.* **2019**, *10*, 1043.
[37] J. Liu, X. Wang, D. Li, N. E. Coates, R. A. Segalman, D. G. Cahill, *Macromolecules* **2015**, *48*, 585.
[38] O. Bubnova, Z. U. Khan, A. Malti, S. Braun, M. Fahlman, M. Berggren, X. Crispin, *Nat. Mater.* **2011**, *10*, 429.
[39] Y. Jia, C. Liu, J. Liu, C. Liu, J. Xu, X. Li, L. Shen, Q. Jiang, X. Wang, J. Yang, F. Jiang, *J. Polym. Sci., Part B: Polym. Phys.* **2019**, *57*, 257.
[40] G. Zotti, S. Zecchin, G. Schiavon, F. Louwet, L. Groenendaal, X. Crispin, W. Osikowicz, W. Salaneck, M. Fahlman, *Macromolecules* **2003**, *36*, 3337.
[41] J. Hynynen, E. Järsvall, R. Kroon, Y. Zhang, S. Barlow, S. R. Marder, M. Kemerink, A. Lund, C. Müller, *ACS Macro Lett.* **2019**, *8*, 70.
[42] A. Lund, S. Darabi, S. Hultmark, J. D. Ryan, B. Andersson, A. Ström, C. Müller, *Adv. Mater. Technol.* **2018**, *3*, 1800251.